Randomness-Induced *XY* Ordering in a Graphene Quantum Hall Ferromagnet

Dmitry A. Abanin, Patrick A. Lee, and Leonid S. Levitov

Department of Physics, Massachusetts Institute of Technology, 77 Massachusetts Avenue, Cambridge, Massachusetts 02139, USA

(Received 2 November 2006; published 10 April 2007)

Valley-polarized quantum Hall states in graphene are described by a Heisenberg O(3) ferromagnet model, with the ordering type controlled by the strength and the sign of the valley anisotropy. A mechanism resulting from electron coupling to the strain-induced gauge field, giving a leading contribution to the anisotropy, is described in terms of an effective random magnetic field aligned with the ferromagnet z axis. We argue that such a random field stabilizes the XY ferromagnet state, which is a coherent equal-weight mixture of the K and K' valley states. The implications such as the Berezinskii-Kosterlitz-Thouless ordering transition and topological defects with half-integer charge are discussed.

DOI: 10.1103/PhysRevLett.98.156801 PACS numbers: 73.43.Nq, 73.43.Lp

Gate-controlled graphene monolayer sheets [1] host an interesting two-dimensional electron system. Recent studies of transport have uncovered, in particular, the anomalous quantum Hall effect [2,3], resulting from the Dirac fermionlike behavior of quasiparticles. Most recently, when the magnetic field was increased above about 20 T, the Landau levels (LL) were found to split [4], with the $n = \pm 1$ and $n = 0$ levels forming two and four sublevels, respectively, as illustrated in Fig. 1(a). The observed splittings were attributed to spin and valley degeneracy lifted by the Zeeman and exchange interactions.

The physics of the interaction-induced gapped quantum Hall state is best understood by analogy with the well-studied quantum Hall bilayers realized in double quantum well systems [5]. In the latter, the interaction is nearly degenerate with respect to rotations of pseudospin describing the two wells. The states with odd filling factors exhibit pseudospin O(3) ordering, the so-called quantum Hall ferromagnet (QHFM) [5]. The pseudospin z component describes density imbalance between the wells, while the x and y components describe the interwell coherence of electron states. Several different phases [6,7] are possible in QHFM depending on the strength of the anisotropic part of Coulomb interaction, controlled by well separation.

In graphene, the two wells correspond to the valleys K and K'. In that, since all electrons are moving in a single plane, the effective interwell separation is of the order of the graphene lattice constant. Crucially, the latter is much smaller than the magnetic length $\ell_B = \sqrt{\hbar c/eB}$. As a result, graphene QHFM can be described as a double-well system with nearly perfect K, K' valley pseudospin symmetry [8–10]. Our estimate [11] (see below) yields anisotropy magnitude of about 10 μK at $B \sim 30$ T, which is very small compared to other energy scales in the system.

Are there other interactions that can break pseudospin symmetry? Coupling to disorder seems an unlikely candidate at first glance. However, there is an interesting effect that has received relatively little attention, which is the strain-induced random gauge field introduced by Iordanskii and Koshelev [12]. To clarify its origin, let us consider the tight-binding model with spatially varying hopping amplitudes. Physically, such a variation can be due to local strain, curvature [13,14], or chemical disorder. With hopping amplitudes t_i for three bond orientations varying independently, we write

$$\varepsilon \begin{pmatrix} u \\ v \end{pmatrix} = \begin{bmatrix} 0 & \tau_{\mathbf{q}} \\ \tau_{\mathbf{q}}^* & 0 \end{bmatrix} \begin{pmatrix} u \\ v \end{pmatrix}, \qquad \tau_{\mathbf{q}} = \sum_{i=1,2,3} t_i e^{i\mathbf{q}\cdot\mathbf{e}_i}, \quad (1)$$

where $\mathbf{e}_i$ are vectors connecting a lattice site to its nearest neighbors, and u and v are wave function amplitudes on the two nonequivalent sublattices A and B. The low-energy Hamiltonian for the valleys K and K' is obtained at $\mathbf{q} \approx \pm\mathbf{q}_0$, the nonequivalent Brillouin zone corners:

$$H_\pm = v \begin{bmatrix} 0 & ip_x \mp p_y + \frac{e}{c} a_\pm \\ -ip_x \mp p_y + \frac{e}{c} a_\pm^* & 0 \end{bmatrix}, \quad (2)$$

with $a_\pm = \frac{c}{e} \sum_{i=1,2,3} \delta t_i e^{\pm i\mathbf{q}_0\cdot\mathbf{e}_i}$, where the subscript $+$ $(-)$ corresponds to the K (K') valley. In writing Eq. (2), we use Cartesian coordinates with the x axis in the armchair

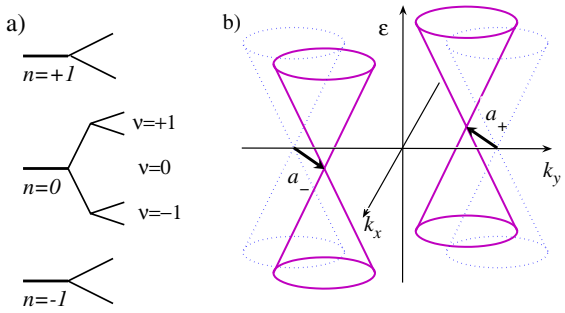

FIG. 1 (color online). (a) Graphene Landau level splitting [4] attributed to spin and valley polarization. When the Zeeman energy exceeds valley anisotropy, all $n = 0$ states are spin-polarized, with the $\nu = \pm 1$ states valley-polarized and the $\nu = 0$ state valley-unpolarized. (b) The effect of uniform strain on the electron spectrum [12] described by the Dirac cones shifting in opposite directions from the points K and K'. Position-dependent strain is described as a random gauge field [Eq. (2)].

direction. Decomposing $a_\pm = a_y \mp i a_x$, we see that the effective vector potential in the two valleys is given by $\pm(a_x, a_y)$. Notably, the gauge field a_μ is of opposite sign for the two valleys, thus preserving time-reversal symmetry [see Fig. 1(b)].

Here we assume that the gauge field has white noise correlations with a correlation length ξ,

$$\langle a_i(k) a_j(k) \rangle_{k\xi \ll 1} = \alpha^2, \qquad a_i(k) = \int e^{-ikr} a_i(r) d^2 r, \tag{3}$$

as appropriate for white noise fluctuations of δt_i. The fluctuating effective magnetic field can be estimated as

$$\delta h(x) = \partial_x a_y - \partial_y a_x \sim \alpha/\xi^2, \tag{4}$$

whereby the correlator of Fourier harmonics $\langle \delta h_k \delta h_{-k} \rangle$ behaves as k^2 at $k\xi \ll 1$.

Recently, a strain-induced effective magnetic field was employed to explain the anomalously small weak localization in graphene [15]. A direct observation of graphene ripples [15] yields typical corrugation length scale ξ of a few tens of nanometers. Estimates from the first principles [15] gave $\delta h \sim 0.1$–1 T, consistent with the observed degree of weak localization suppression.

Valley anisotropy of coupling to the gauge field [Eq. (2)] generates a uniaxial random Zeeman-like interaction $\delta h \sigma_3$ for the K-K' pseudospin order parameter. We shall see that, somewhat counterintuitively, weak δh induces ordering in the system, acting as an easy-plane anisotropy which favors the XY state. This behavior can be understood by noting that the transverse fluctuations in a ferromagnet are softer than the longitudinal fluctuations, making it beneficial for the spins to be polarized, on average, transversely to the field, as illustrated in Fig. 2. This *random field-induced ordering* maximizes the energy gain of the spin system coupled to δh.

For magnets with a uniaxial random field, this behavior has been established [16,17] in the high space dimension. The situation in dimension two is more delicate [18,19] due to competition with the Larkin-Imry-Ma (LIM) [20,21] disordered state. We shall see that the anisotropy induced by a random gauge field is considerably more robust than that due to a random magnetic field. (The proposed scenario of randomness-induced order is also relevant for the two-valley QH in the AlAs system [22].)

The field-induced easy-plane anisotropy completely changes thermodynamics, transforming an O(3) ferromagnet, which does not order in 2D, to the XY model, which exhibits a Berezinskii-Kosterlitz-Thouless (BKT) transition to an ordered XY state. The transition temperature T_{BKT} is logarithmically renormalized by the out-of-plane fluctuations [23]:

$$T_{\mathrm{BKT}} \sim J/\ln(l_{XY}/\ell_B), \qquad \ell_B = (\hbar c/eB)^{1/2}, \tag{5}$$

where l_{XY} is the correlation length. For fields $B \sim 30$ T,

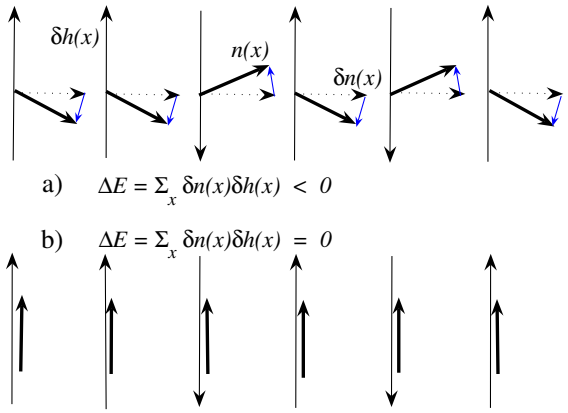

FIG. 2 (color online). Random field-induced order in a ferromagnet. The energy gained from the order parameter tilting opposite to the field is (a) maximal when the spins and the field are perpendicular and (b) minimal when they are parallel. Uniaxial random field induces XY ordering in the transverse plane.

with l_{XY} given by Eq. (16) below, we obtain T_{BKT} in the experimentally accessible range of a few degrees Kelvin.

The XY-ordered QHFM state hosts fractional $\pm e/2$ charge excitations, so-called merons [7]. Merons are vortices such that in the vortex core the order parameter smoothly rotates out of the xy plane. There are four types of merons [7], since a meron can have positive or negative vorticity, and the order parameter inside the core can tilt in either the $+z$ or the $-z$ direction. A pair of merons with the same charge and opposite vorticity is topologically equivalent to a skyrmion of charge $2(e/2) = e$ [7].

In graphene QHFM, the hierarchy of the spin- and valley-polarized states is determined by the relative strength of the Zeeman energy and the randomness-induced anisotropy. Our estimate below obtains the anisotropy of a few degrees Kelvin at $B \sim 30$ T. This is smaller than the Zeeman energy in graphene $\Delta_{\mathrm{Z}} = g\mu_B B \sim 50$ K at $B \sim 30$ T. Therefore, we expect that $\nu = 0$ state is spin-polarized, with both valley states filled. (This was assumed in our previous analysis [24] of edge states in the $\nu = 0$ state.) In contrast, in highly corrugated samples, when the anisotropy exceeds the Zeeman energy, an easy-plane valley-polarized $\nu = 0$ state can be favored.

While the character of the $\nu = 0$ state is sensitive to the anisotropy strength, the $\nu = \pm 1$ states [see Fig. 1(a)] are always both spin- and valley-polarized. Below, we focus on $\nu = \pm 1$ states, keeping in mind that for strong randomness our discussion also applies to the $\nu = 0$ state.

Zeeman-split free Dirac fermion LL are given by

$$E_n = \mathrm{sgn}(n)\sqrt{|2n|}\frac{\hbar v}{\ell_B} \pm \frac{1}{2}\Delta_{\mathrm{Z}}, \tag{6}$$

with n an integer and $v \approx 8 \times 10^7$ cm/s. Each LL is doubly valley-degenerate. The random field (4) couples to the electron orbital motion in the same way as the external field B, producing a local change in cyclotron energy and in the LL density. While the random field splits

the $n \neq 0$ LL, for $n = 0$, it does not affect the single-particle energy (6) and couples to electron dynamics via exchange effects only. To estimate this coupling, we note that the field (4) leads to valley imbalance in exchange energy per particle [Eq. (8) in Ref. [24]]:

$$E_{K(K')} = E_{\text{exch}}(B \pm \delta h) = \frac{Ae^2}{\kappa \ell_{B \pm \delta h}}, \qquad A = \left(\frac{\pi}{8}\right)^{1/2}, \quad (7)$$

where $\kappa \approx 5.24$ is the dielectric constant of graphene.

Let us analyze the graphene QHFM energy dependence on the gauge field. We consider a fully spin- and valley-polarized $\nu = -1$ state, described by a ferromagnetic order parameter $\mathbf{n} = (n_1, n_2, n_3)$ in the K, K' valley space. The valley-isotropic exchange interaction gives rise to a sigma model, with the gradient term only [6]:

$$E_0(n) = \frac{1}{2} \int J(\nabla \mathbf{n})^2 d^2x, \qquad J = \frac{e^2}{64\kappa \ell_B}. \quad (8)$$

The valley-asymmetric coupling to δh in Eq. (7) generates a Zeeman-like Hamiltonian with a uniaxial random field:

$$E_1(n) = \int g \delta h(x) n_3(x) d^2x, \qquad g = n \frac{dE_{\text{exch}}}{dB} = \frac{Ane^2}{2B\kappa \ell_B}, \quad (9)$$

where $n = 1/2\pi\ell_B^2$ is the electron density.

We estimate the energy gain from the order parameter $\mathbf{n}(x)$ correlations with the random field, treating the anisotropy (9) perturbatively in δh. Decomposing $\mathbf{n}(x) = \bar{\mathbf{n}} + \delta\mathbf{n}(x)$ and taking variation in $\delta\mathbf{n}$, we obtain

$$J\nabla^2 \delta\mathbf{n} = g\delta\mathbf{h}_\perp, \qquad \delta\mathbf{h}_\perp = [\mathbf{z} - \bar{\mathbf{n}}(\bar{\mathbf{n}} \cdot \mathbf{z})]\delta h.$$

Substituting the solution for $\delta\mathbf{n}$ into the energy functional (8) and (9), we find an energy gain for $\bar{\mathbf{n}}$ of the form

$$\delta E = -\lambda \int [1 - \bar{n}_3^2(x)] d^2x, \qquad \lambda = \sum_k \frac{g^2 \langle \delta h_{-k} \delta h_k \rangle}{2Jk^2}, \quad (10)$$

where averaging over spatial fluctuations of δh is performed. This anisotropy favors the XY state $\bar{n}_3 = 0$. As illustrated in Fig. 2, the fluctuations due to $\delta\mathbf{n}$ tilting towards the z axis minimize the energy of coupling to the uniaxial field when $\bar{\mathbf{n}}$ is transverse to it.

Now let us compare the energies of the XY and the Larkin-Imry-Ma state [20,21]. In the LIM state, the energy is lowered by domain formation such that the order parameter in each domain is aligned with the average field in this domain. Polarization varies smoothly between domains, and the typical domain size L is determined by the balance between domain wall and magnetic field energies. In our system, the LIM energy per unit area is

$$\varepsilon_{\text{LIM}} \sim -\frac{g\Phi(L)}{L^2} + \frac{J}{L^2}, \quad (11)$$

where $\Phi(L)$ is a typical flux value through a region of size L. To estimate $\Phi(L)$, we write the magnetic flux through a region of size L as an integral of the vector potential over the boundary, which gives

$$\Phi(L) = \oint a_i(x) dx_i \sim \alpha\sqrt{L/\xi}. \quad (12)$$

Minimizing the LIM energy (11), we find

$$\varepsilon_{\text{LIM}} \sim -\frac{g^4\alpha^4}{J^3\xi^2}. \quad (13)$$

Comparison to the XY anisotropy $\lambda \sim -g^2\alpha^2/J\xi^2$ gives

$$\frac{\lambda}{\varepsilon_{\text{LIM}}} \sim \frac{J^2}{g^2\alpha^2} \sim \left(\frac{\Phi_0}{\Phi(\xi)}\right)^2, \qquad \Phi_0 = hc/e, \quad (14)$$

where $\Phi(\xi) \sim \alpha$ is the flux through a region of size ξ. Interestingly, the ratio (14) does not depend on the external magnetic field. Therefore, at weak randomness, when the random field flux through an area ξ^2 is much smaller than Φ_0, the ordered XY state has lower energy than the disordered LIM state.

In the opposite limit of strong randomness, spins align with the local δh, forming a disordered state. It is instructive to note that, for a model with white noise correlations of magnetic field rather than of vector potential, the ratio (14) is of order one. In this case, the competition of the LIM and the ordered states is more delicate.

A different perspective on the random-field-induced ordering is provided by analogy with the classical dynamics of a pendulum driven at suspension [25]. The latter, when driven at a sufficiently high frequency, acquires a steady state with the pendulum pointing along the driving force axis. As discussed in Ref. [26], this phenomenon can be described by an effective potential U_{eff} obtained by averaging the kinetic energy over fast oscillations, with the minima of U_{eff} on the driving axis and maxima in the equatorial plane perpendicular to it. This behavior is robust upon replacement of periodic driving by noise [27]. Our statistical-mechanical problem differs from the pendulum problem merely in that the 1D time axis is replaced by 2D position space, which is inessential for the validity of the argument. The resulting effective potential is thus identical to that for the pendulum, with the only caveat being the sign change $U_{\text{eff}} \to -U_{\text{eff}}$ in the effective action, as appropriate for a transition from classical to statistical mechanics. Thus, in our case the minima of U_{eff} are found in the equatorial plane, in agreement with the above discussion.

The easy-plane anisotropy (10) can be estimated as

$$\lambda/n \sim \frac{\delta h^2}{B^2} \frac{\xi^2}{\ell_B^2} \frac{e^2}{\kappa \ell_B} \approx 0.1\text{–}10 \text{ K/particle}, \quad (15)$$

where $\delta h \sim 0.1$–1 T, $\xi \sim 30$ nm, and $B \sim 30$ T was used. Since this is smaller than the Zeeman energy, we expect that the easy-plane ferromagnet in the valley space is realized at $\nu = \pm 1$, while the $\nu = 0$ state is spin-polarized with both valley states filled.

The out-of-plane fluctuations of the order parameter are characterized by the correlation length

$$l_{XY} \sim \sqrt{J/\lambda} \approx 1\text{–}10\ell_B \tag{16}$$

for the above parameter values. The length l_{XY} sets a typical scale for an order parameter change in the core of vortices (merons) as well as near edges of the sample and defects which induce the nonzero z component.

To measure the correlation length l_{XY}, one may use the spatial structure of the $\nu = 0$ wave function. Since the $K(K')$ electrons reside solely on either the B or the A sublattice, the order parameter z component is equal to the density imbalance between the two sublattices. The latter can be directly measured by the STM imaging technique. For the temperature of XY ordering [Eq. (5)] with J estimated from (8), we obtain T_{BKT} on a few degrees Kelvin scale.

This should be compared to the intrinsic QHFM valley anisotropy of a pure graphene sheet. In the zeroth LL, the K-K' superposition states have a somewhat different density distribution than the valley-polarized states, since for each valley the zeroth LL occupies just one sublattice (A for K', B for K). In particular, electrons occupy both sublattices equally in the state with the order parameter in the xy plane. This leads to a dependence of the QHFM Coulomb energy on the orientation of the order parameter. This anisotropy, estimated using the Hartree-Fock approximation [11], was found to be

$$\Delta E \approx -\frac{27}{512\pi^3}\left(\frac{a}{\ell_B}\right)^3 \frac{e^2}{\kappa\ell_B} \sim 10\ \mu\mathrm{K}, \tag{17}$$

indicating that the anisotropy is negligible.

We note that the situation is completely different for higher LL. Goerbig *et al.* [9] pointed out that the Coulomb interaction can backscatter electrons of K and K' type at LL with $n \neq 0$, which leads to a much stronger lattice anisotropy of the order a/l_B. This effect is absent for the zeroth LL due to the fact that K and K' states occupy different sublattices.

In summary, there are several competing mechanisms of valley symmetry breaking in graphene QHFM. We considered the coupling of the strain-induced random magnetic field and found that it generates an easy-plane anisotropy, which is much stronger than the symmetry-breaking terms due to lattice. The estimates of the field-induced anisotropy suggest that the random field may be a principal mechanism of K-K' QHFM symmetry breaking. The easy-plane ordered state is expected to exhibit a BKT transition at experimentally accessible temperatures and half-integer charge excitations.

We are grateful to A. K. Geim, M. Kardar, and P. Kim for useful discussions. This work is supported by the NSF MRSEC Program (No. DMR 02132802), NSF-NIRT No. DMR-0304019 (D. A., L. L.), and NSF Grant No. DMR-0517222 (P. L.).

[1] K. S. Novoselov, A. K. Geim, S. V. Morozov, D. Jiang, Y. Zhang, S. V. Dubonos, I. V. Grigorieva, and A. A. Firsov, Science **306**, 666 (2004); Proc. Natl. Acad. Sci. U.S.A. **102**, 10 451 (2005).
[2] K. S. Novoselov, A. K. Geim, S. V. Morozov, D. Jiang, M. I. Katsnelson, I. V. Grigorieva, S. V. Dubonos, and A. A. Firsov, Nature (London) **438**, 197 (2005).
[3] Y. Zhang, Y.-W. Tan, H. L. Stormer, and P. Kim, Nature (London) **438**, 201 (2005).
[4] Y. Zhang, Z. Jiang, J. P. Small, M. S. Purewal, Y. W. Tan, M. Fazlollahi, J. D. Chudow, J. A. Jaszaczak, H. L. Stormer, and P. Kim, Phys. Rev. Lett. **96**, 136806 (2006).
[5] For a review, see S. M. Girvin and A. H. MacDonald, in *Perspectives in Quantum-Hall Effects*, edited by S. Das Sarma and A. Pinczuk (Wiley, New York, 1997).
[6] K. Yang, K. Moon, L. Zheng, A. H. MacDonald, S. M. Girvin, D. Yoshioka, and S.-C. Zhang, Phys. Rev. Lett. **72**, 732 (1994).
[7] K. Moon, H. Mori, K. Yang, S. M. Girvin, A. H. MacDonald, L. Zheng, D. Yoshioka, and S.-C. Zhang, Phys. Rev. B **51**, 5138 (1995).
[8] K. Nomura and A. H. MacDonald, Phys. Rev. Lett. **96**, 256602 (2006).
[9] M. O. Goerbig, R. Moessner, and B. Douçot, Phys. Rev. B **74**, 161407 (2006).
[10] J. Alicea and M. P. A. Fisher, Phys. Rev. B **74**, 075422 (2006).
[11] D. A. Abanin, P. A. Lee, and L. S. Levitov, cond-mat/0611062; see discussion preceding Eq. (17).
[12] S. V. Iordanskii and A. E. Koshelev, Pis'ma Zh. Eksp. Teor. Fiz. **41**, 471 (1985) [JETP Lett. **41**, 574 (1985)].
[13] C. L. Kane and E. J. Mele, Phys. Rev. Lett. **78**, 1932 (1997).
[14] A. Morpurgo and F. Guinea, Phys. Rev. Lett. **97**, 196804 (2006).
[15] S. V. Morozov, K. S. Novoselov, M. I. Katsnelson, F. Schedin, L. A. Ponomarenko, D. Jiang, and A. K. Geim, Phys. Rev. Lett. **97**, 016801 (2006).
[16] A. Aharony, Phys. Rev. B **18**, 3328 (1978).
[17] D. E. Feldman, J. Phys. A **31**, L177 (1998).
[18] B. J. Minchau and R. A. Pelcovits, Phys. Rev. B **32**, 3081 (1985).
[19] J. Wehr, A. Niederberger, L. Sanchez-Palencia, and M. Lewenstein, Phys. Rev. B **74**, 224448 (2006).
[20] A. I. Larkin, JETP **31**, 784 (1970).
[21] Y. Imry and S. K. Ma, Phys. Rev. Lett. **35**, 1399 (1975).
[22] Y. P. Shkolnikov, S. Misra, N. C. Bishop, E. P. De Poortere, and M. Shayegan, Phys. Rev. Lett. **95**, 066809 (2005).
[23] S. Hikami and T. Tsuneto, Prog. Theor. Phys. **63**, 387 (1980).
[24] D. A. Abanin, P. A. Lee, and L. S. Levitov, Phys. Rev. Lett. **96**, 176803 (2006).
[25] P. L. Kapitza, Zh. Eksp. Teor. Fiz. **21**, 588 (1951).
[26] L. D. Landau and E. M. Lifshitz, *Mechanics* (Reed Educational and Professional Publishing, Oxford, England, 2002), Chap. V, Sec. 30.
[27] R. L. Stratonovich and Yu. M. Romanovsky, Nauchn. Dokl. Vyss. Sk. **3**, 221 (1958) (in Russian).